MicroRNA is a potential target for therapies to improve the physiological function of skeletal muscle after trauma

https://doi.org/10.4103/1673-5374.330620

Date of submission: May 20, 2021

Date of decision: July 6, 2021

Date of acceptance: September 23, 2021

Date of web publication: December 10, 2021

Xin-Yi Gu[1, 2, #], Bo Jin[3, #], Zhi-Dan Qi[1, 2], Xiao-Feng Yin[1, 2, *]

From the Contents

Introduction	1617
Materials and Methods	1618
Results	1619
Discussion	1621

Graphical Abstract *The changes of miR-142a-3p expression can affect the ion channel currents of C2C12, suggesting effects on muscle cell electrophysiology*

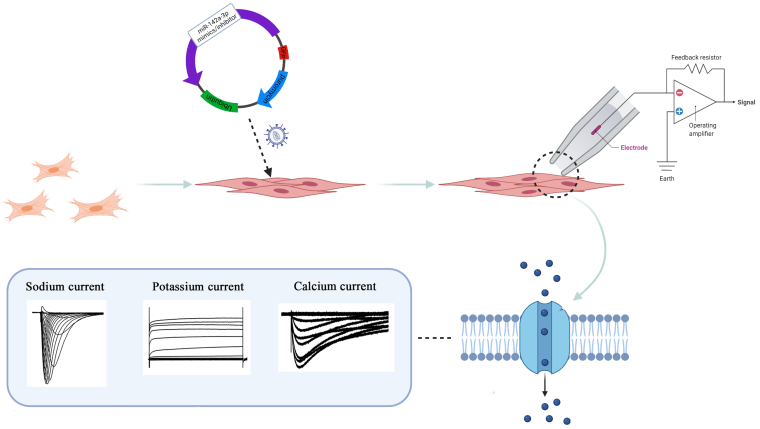

Abstract

MicroRNAs can regulate the function of ion channels in many organs. Based on our previous study we propose that miR-142a-39, which is highly expressed in denervated skeletal muscle, might affect cell excitability through similar mechanisms. In this study, we overexpressed or knocked down miR-142a-3p in C2C12 cells using a lentivirus method. After 7 days of differentiation culture, whole-cell currents were recorded. The results showed that overexpression of miR-142a-3p reduced the cell membrane capacitance, increased potassium current density and decreased calcium current density. Knockdown of miR-142a-3p reduced sodium ion channel current density. The results showed that change in miR-142a-3p expression affected the ion channel currents in C2C12 cells, suggesting its possible roles in muscle cell electrophysiology. This study was approved by the Animal Ethics Committee of Peking University in July 2020 (approval No. LA2017128).

Key Words: C2C12; denervation; ion channels; microRNA; miR-142a-3p; muscle; patch clamp; potassium; sodium; whole-cell currents

Chinese Library Classification No. R446; R741; R318

Introduction

Since miR-1 was first studied as a cardiac electrophysiological regulator in 2007 (Yang et al., 2007), a large number of studies have confirmed the role of microRNAs (miRNAs) in regulating ion channels in the cardiovascular system, nervous system, endocrine and cancer biology (Baroukh et al., 2007; Yang et al., 2007; Pardo and Stühmer, 2008; Saugstad, 2010). miRNAs can regulate cell electrophysiology by directly targeting mRNAs coding ion channels and transporters or indirectly regulating ion channel expression by targeting transcription factors (Pietrzykowski et al., 2008; Shi et al., 2009; Manna et al., 2021; Zeng et al., 2021). In addition, miRNA may indirectly affect ion channel function by targeting proteins that interact with channels, thereby enhancing the complexity and fine regulation of miRNA interactions. Skeletal muscle cells are excitable cells, therefore the expression changes of ion channels in muscle can lead to various diseases, affect cell excitability and electrical conduction and alter normal physiological function (Arnolds et al., 2012; Liu et al., 2015). miRNAs have powerful regulatory potential for skeletal muscle electrophysiology, but so far there have been relatively few related studies.

miR-142a-3p was one of the miRNAs with the most significant different expression in mouse skeletal muscle after denervation (Weng et al., 2018). It has been regarded as the main regulator of cell fate in the hematopoietic system (Nimmo et al., 2013) and plays a role in virus infection,

[1]Department of Orthopedics and Traumatology, Peking University People's Hospital, Beijing, China; [2]Key Laboratory of Trauma and Neural Regeneration (Peking University), Beijing, China; [3]Department of Orthopedics, The First Affiliated Hospital of Nanjing Medical University, Jiangsu Province Hospital, Nanjing, Jiangsu Province, China

*Correspondence to: Xiao-Feng Yin, MD, PhD, xiaofengyin@bjmu.edu.cn.

https://orcid.org/0000-0001-9932-642X (Xiao-Feng Yin)

#Both authors contributed equally to this paper.

Funding: *This study was supported by the National Natural Science Foundation of China, Nos. 82072162, 81971177); and Beijing Municipal Natural Science Foundation of China, No. 7192215 (all to XFY).*

How to cite this article: *Gu XY, Jin B, Qi ZD, Yin XF (2022) MicroRNA is a potential target for therapies to improve the physiological function of skeletal muscle after trauma. Neural Regen Res 17(7):1617-1622.*

inflammation and cancer (Kaduthanam et al., 2013; Kramer et al., 2015; Mandolesi et al., 2017). It also has been found that miR-142a-3p can inhibit the utilization of lipid in skeletal muscle and complements the effects of miR-27a-3p in the regulation of muscle fiber metabolism (Chemello et al., 2019). Shrestha et al. (2015) predicted and analyzed the targets of miR-142a-3p and found that miR-142a-3p may affect the regulation of the actin cytoskeleton. However, the effect of miR-142a-3p on the electrophysiology of skeletal muscle has not been explored.

Recently we confirmed that another miRNA, miR-34c-5p, is also overexpressed in denervation skeletal muscle and regulates the electrophysiology of C2C12 cells, which suggests the importance of miRNAs in regulating skeletal muscle ion channel currents (Jin et al., 2020). This further sparked our interest in miR-142a-3p. Differently expressed genes and miR-142a-3p predicted target genes were cross-labeled, and the gene oncology analysis showed that the target genes of miR-142a-3p participate highly in metal binding, cation binding, ion binding in binding gene oncology terms (**Additional Figure 1**). miR-142a-3p was also predicted by MR-microT (www.microrna.gr/microT) to regulate gene expression (*Scn4a*, *Scn5a*, *Kcna2*, *Kcnc1*, *Cacna2d1*) of many ion channels (**Table 1**). All these findings indicate that miR-142a-3p may have an important effect on skeletal muscle ion channels.

Table 1 | **Predictive targets of miR-142a-3p by MR-microT**

Gene ID	Gene name	Channel type	Gene description
ENSMUSG00000001027	*Scn4a*	Sodium	Voltage-gated, type IV, alpha
ENSMUSG00000032511	*Scn5a*	Sodium	Voltage-gated, type V, alpha
ENSMUST00000038695	*Kcna2*	Potassium	Voltage-gated channel, shaker-related subfamily, member 2
ENSMUST00000025202	*Kcnc1*	Potassium	Voltage-gated channel, Shaw-related subfamily, member 1
ENSMUSG00000040118	*Cacna2d1*	Calcium	Calcium channel, voltage-dependent, alpha2/delta subunit 1

To investigate those results further, we established C2C12 cell models of miR-142a-3p overexpression, knockdown and control groups by lentivirus. We recorded their cell membrane capacitance and various ion channel currents of each group to explore the regulatory function of miR-142a-3p on the electrophysiology of C2C12 cells.

Materials and Methods

Cell culture

C2C12 cell line (RRID: CVCL_0188) was purchased from the American Type Culture Collection (Atlanta, MD, USA) and identified by STR. The cells were cultured at 37°C, 5% CO_2, and the growth medium (GM) was changed every three days. The GM consists of Dulbecco's modified Eagle's medium with 10% fetal bovine serum (Gibco, New York, NY, USA) and 1% penicillin/streptomycin (Gibco).

C2C12 myotube differentiation

After the cells were cultured at equal density, the GM was replaced by the differentiation medium. The differentiation medium consists of Dulbecco's modified Eagle's medium with 2% horse serum (Biological Industries, Beit Haemek, Israel) and 1% penicillin/streptomycin. The differentiation medium was changed every 3 days, and the cells were collected on the 7^{th} day for the subsequent experiments (Kubo, 1991).

Plasmid construction and cell transfection

In this experiment, miR-142a-3p overexpression, knockdown and control groups were constructed using the plasmid hU6-MCS-Ubiquitin-EGFP-IRES-puromycin (Genechem, Shanghai, China). Lentivirus (Genechem) was used to package the plasmid, and finally used to transfect cells. The method is as follows: the vector and the target fragment were each digested with the same restriction enzymes (Beyotime, Shanghai, China) and, after agarose electrophoresis, the gel was cut to recover the product. The recovered vector and the target fragment were ligated overnight at 16°C; the ligation product was used to transform Escherichia coli. The Plasmid Midi Preparation Kit (Beyotime) was used to extract the plasmids.

The cells were planted in a 24-well plate at a density of 30–50%, and GM, lentiviral infection enhancing reagent (Genechem) and 1.5×10^7 TU/mL lentivirus were added sequentially. The total volume was 500 µL. After 72 hours of culture, the culture medium was replaced with GM and the transfection efficiency was observed under a fluorescence microscope (MZ75, Leica, Bensheim, Germany). Cells expressing green fluorescent protein were deemed to be successfully transfected. The cell transfection rate was calculated as the number of green fluorescent cells/total cells.

Muscle sampling

To exclude the interference of the physiological cycle and hormone secretion in female animals, nine healthy male C57BL/6 mice (specific pathogen free, 6–8 weeks, 22–25 g; purchased by Charles River, Boston, MA, USA) were used in this study. The study was approved by the Animal Ethics Committee of Peking University in July 2020 (approval No. LA2017128).

Each experimental animal was anesthetized with 1.5% isoflurane (Huazhong Haiwei (Beijing) Gene Technology Co., Ltd., Beijing, China). After anesthesia, the right lower limb of the experimental animal was shaved, and the skin was disinfected with iodophor (Shandong Likang Medical Equipment Technology Co., Ltd., Linyi, China). An incision was made and the gastrocnemius muscle of the right lower limb of the mouse was completely separated from the Achilles tendon to the knee joint for measurement and comparison. The gastrocnemius muscle of the right lower extremity was harvested at 0, 1 or 2 weeks after surgery.

Quantitative real-time polymerase chain reaction

TRIzol reagent (Invitrogen, Carlsbad, CA, USA) was used to extract total RNA from the gastrocnemius muscle according to the manufacturer's instructions. 5X All-In-One RT MasterMix Kit (Abm, Vancouver, Canada) was used to reverse transcribe RNA into DNA. The Bio-Rad iQTM5 system (Bio-Rad, Mississauga, Canada) was used to perform quantitative real-time reverse transcription-polymerase chain reaction (qRT-PCR) and the qRT-PCR data was analyzed by $2^{-\Delta\Delta Ct}$ method (Livak Method). Mouse glyceraldehyde-3-phosphate dehydrogenase (GAPDH) was the reference gene in this experiment, and the gene primer sequences are listed in **Table 2**.

Electrophysiology

Electrode preparation and experiment recording

The whole-cell patch clamp solution formulae for sodium current (I_{Na}), potassium current (I_{Kd}) and L-type calcium current ($I_{Ca,L}$) were in accordance with a study by Nakada et al. (2018), as shown in **Table 3**.

Table 2 | **Primer sequence**

	Primer sequence
miR-142a-3p	Reverse transcription primer: 5′-CTC AAC TGG TGT CGT GGA GTC GGC AAT TCA GTT GAG TCC ATA AA-3′
	Forward primer: 5′-ATC GTC GTC CGT GTA GTG TTT CC TAC-3′
	Reverse primer: 5′-CTC AAC TGG TGT CGT GGA GTC-3′
U6	Reverse transcription primer: 5′-AAC GCT TCA CGA ATT GCG T-3′
	Forward primer: 5′-CTC GCT TCG GCA GCA A-3′
	Reverse primer: 5′-AAC GCT TCA CGA ATT GCG T-3′
GAPDH	Forward primer: 5′-GGC CGC CTG GAG AAA CCT-3′
	Reverse primer: 5′-AAG TCG CAG GAG ACA ACC-3′
Scn4a	Forward primer: 5′-TCT TGT CTA GCA GGC AGC ATC G-3′
	Reverse primer: 5′-CCA GGC ACA GTC CCA GAT TCA A-3′
Scn5a	Forward primer: 5′-TCC GCG TCT CTG TGT GGA AG-3′
	Reverse primer: 5′-CGA GTT CTG GCA CCT CCG TT-3′
Kcna2	Forward primer: 5′-CTG CAA GGG CAA CGT CAC AC-3′
	Reverse primer: 5′-GGG ACA GTG AGA TGC TTG GC-3′
Kcnc1	Forward primer: 5′-ACG GCA GTC AGT CAT CGG TCA-3′
	Reverse primer: 5′-TGG AAG AGG GTG GCA GTG TGA A-3′
Cacna2d1	Forward primer: 5′-GCA GCC CAG ATA CCG AAA AG-3′
	Reverse primer: 5′-TCG TTG CAG ATC TGG GTT CT-3′

Cacna2d1: Calcium voltage-gated channel auxiliary subunit alpha2delta 1; GAPDH: glyceraldehyde-3-phosphate dehydrogenase; Kcna2: potassium voltage-gated channel subfamily A member 2; Kcnc1: potassium voltage-gated channel subfamily C member 1; Scn4a: sodium voltage-gated channel alpha subunit 4.

Table 3 | **Whole-cell patch clamp solution formulae**

	Extracellular solution (in mM)	Solution in borosilicate glass pipettes (in mM)
Sodium current (I_{Na})	80 CsCl, 70 NaCl, 5.4 KCl, 2 $CaCl_2$, 1 $MgCl_2$•$6H_2O$, 10 HEPES, 10 glocose (pH to 7.4 with CsOH)	40 CsF, 100 CsCl, 2 TEA, 2 $MgCl_2$•$6H_2O$, 10 HEPES, 10 EGTA (pH to 7.3 with CsOH)
Potassium current (I_{Kd})	140 NaCl, 5 KCl, 2 $CaCl_2$, 1 $MgCl_2$•$6H_2O$, 10 HEPES, 10 glocose, 0.3 $CdCl_2$ (pH to 7.4 with NaOH)	10 KCl, 120 K-glutamate, 5 EGTA, 10 HEPES, 5 MgATP (pH to 7.3 with KOH)
L-type calcium current ($I_{Ca,L}$)	145 TEACl, 10 $CaCl_2$, 10 HEPES, 5.5 glucose (pH to 7.4 with TEAOH)	145 D-glutamic acid, 0.1 EGTA, 2 MgATP, 10 HEPES, 2 $MgCl_2$•$6H_2O$ (pH to 7.3 with CsOH)

EGTA: Ethylene glycol tetraacetic acid; HEPES: 4-(2-hydroxyethyl)-1-piperazineethanesulfonic acid; TEA: trimethylamine.

The borosilicate capillary glass was placed in a PC-10 Puller (Narishige, Tokyo, Japan) and stretched through a two-step process. After filling the inner liquid, the resistance of borosilicate capillary glass was 3–5 MΩ. Vacuum suction was applied to complete the Giga-ohm seal, and then negative pressure was released to rupture the cell membrane. The series resistance was between 4–7 MΩ, and the compensation was 70–90%. Digidata 1440A and MultiClamp 700B hardware were used for the experimental recordings. Clampex 10.6 and MultiClamp 700B command software were used for data acquisition. The above hardware and software were provided by Molecular Device-Axon Instruments (San Jose, CA, USA).

Stimulus waveform and membrane capacitance recording

Recordings were made from C2C12 myotubes in each experimental group. I_{Na} were elicited by a series of 20 ms lasting depolarizations from a –120 mV holding potential to voltage ranging from a program of –80 to +20 mV in 5 mV steps. I_{Kd} were induced by the following protocol: a holding potential at –80 mV for 10 ms, then changing to a series of depolarizing steps from –100 to +80 mV in 20 mV increments and then returning to –60 mV, were used to obtain the I_{Kd} current density curve. The $I_{Ca,L}$ stimulation square wave was as follows: the initial voltage was maintained at –80 mV, then rose to –40 mV for 1 second, after that, rose to –60 to +70 mV (step 10 mV) for 2 seconds, and finally held at –80 mV for 7 seconds (Beam et al., 1986). The capacitance was compensated and recorded, and the compensation mode was 100% compensation. The cell membrane capacitances of each group was then counted.

Statistical analysis

Clampfit 10.6 (Molecular Devices, San Jose, CA, USA) and OriginPro 2019 (OriginLab, Northampton, MA, USA) were used. Significant differences were determined using a two-tailed Student's *t*-test and data are expressed as mean ± standard error of mean (SEM). A probability value of $P < 0.05$ was considered statistically significant.

Results

miR-142a-3p expression and transfection efficiency

The expression of miR-142a-3p was detected by qRT-PCR at 0, 1 and 2 weeks after sciatic nerve excision. The miR-142a-3p expression had significantly increased by the 2nd week after injury ($P < 0.01$, *vs.* 0 week, **Figure 1A**). The transfected cells were screened with puromycin, then qRT-PCR was used to verify the expression of miR-142a-3p in each group of cells (**Figure 1B**). At each time, the transfection efficiency was recorded under a microscope. The cells with green fluorescence were regarded as successful transfection cells. The transfection efficiency in each group was ~0.9 (**Figure 1C** and **D**).

Effects of miR-142a-3p on the voltage-gated sodium, potassium and calcium channel currents in C2C12 myotubes

After 7 days of differentiation, the membrane capacitance of each group was calculated. Compared with the negative control (NC) group, the membrane capacitance in the miR-142a-3p overexpression group was down-regulated ($P < 0.01$), and the membrane capacitance of miR-142a-3p knockdown group was up-regulated ($P < 0.01$) (**Figure 2**).

In the miR-142a-3p overexpression group, the peak currents density of the I_{Na} did not change significantly ($P = 0.53$, *vs*. NC group), whereas, in the miR-142a-3p knockdown group, the peak currents density of the I_{Na} was lower than in the control group ($P < 0.05$, *vs*. NC group) (**Figure 3**).

In the miR-142a-3p overexpression group, the peak currents density of the I_{Kd} was higher than in the control group ($P < 0.05$, *vs*. NC group), however, there was no significant change in the peak currents density of the I_{Kd} in the miR-142a-3p knockdown group($P = 0.34$, *vs*. NC group) (**Figure 4**).

In the miR-142a-3p overexpression group, the peak currents density of the $I_{Ca,L}$ decreased relative to the control group ($P < 0.05$, *vs*. NC group), whereas in the miR-142a-3p knockdown group, the peak currents density of the $I_{Ca,L}$ did not change significantly ($P = 0.12$, *vs*. NC group) (**Figure 5**).

Prediction of ion channel-related targets of miR-142a-3p

We predicted the ion channel-related targets of miR-142a-3p by MR-microT, and found its potential regulatory targets *Scn4a*, *Scn5a*, *Kcna2*, *Kcnc1*, and *Cacna2d1* (**Table 1**). The cells in each group were differentiated for 7 days. qRT-PCR results showed that *Scn4a*, *Scn5a*, *Kcna2*, and *Cacna2d1* were significantly down-regulated in the miR-142a-3p overexpression group ($P < 0.05$, *vs*. NC group), and up-regulated in the miR-142a-3p knockdown group ($P < 0.05$, *vs*. NC group) compared with the control group (**Figure 6**).

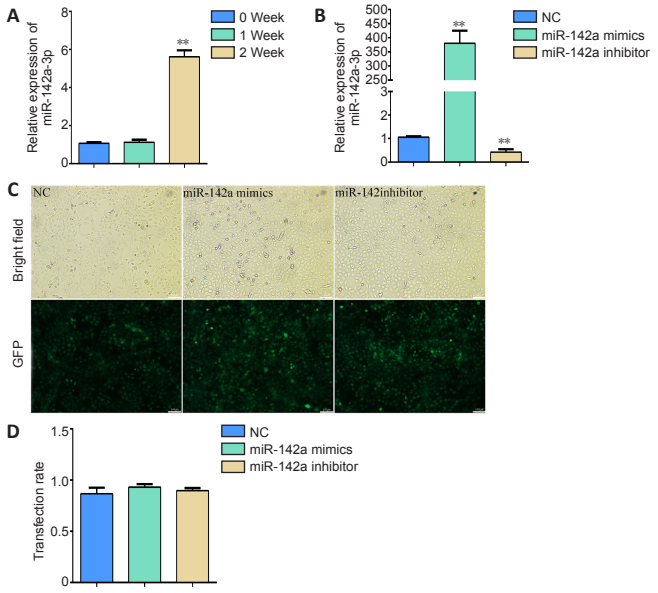

Figure 1 | Detection of miR-142a-3p in denervated muscle and establishment of cell models.
(A, B) Quantitative real-time reverse transcription-polymerase chain reaction was implemented to detect the expression of miR-142a-3p in gastrocnemius muscle (A) and differently treated cells (B). Relative expression of miR-142a-3p was normalized by fold change. (C) Cell transfection was observed under a fluorescence microscope. Cells expressing green fluorescent protein were deemed to be successfully transfected. Scale bars: 100 μm. (D) Cell transfection rate was calculated by the number of green fluorescent cells/total cells. Data are expressed as mean ± SEM (n = 3/group). *P < 0.05, **P < 0.01, *vs.* NC (two-tailed Student's t-test). GFP: Green fluorescent protein; miR-142a inhibitor: miR-142a-3p knockdown group; miR-142a mimics: miR-142a-3p overexpression group; NC: negative control group.

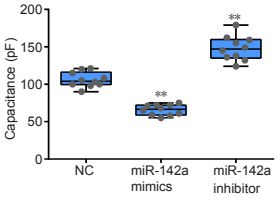

Figure 2 | Cell membrane capacitance in miR-142a-3p overexpression and knockdown C2C12 cells.
Data are expressed as mean ± SEM (n = 10/group). **P <0.01, *vs.* NC group (two-tailed Student's t-test). miR-142a inhibitor: miR-142a-3p knockdown group; miR-142a mimics: miR-142a-3p overexpression group; NC: negative control group.

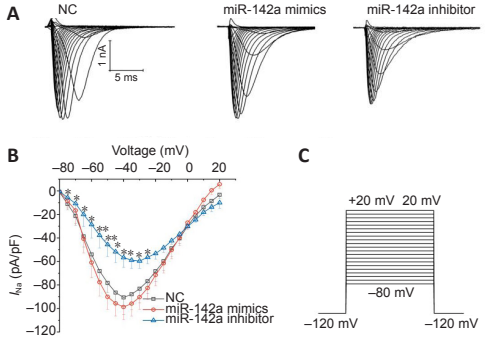

Figure 3 | Knockdown of miR-142a-3p decreases the whole-cell voltage-gated sodium channel currents (I_{Na}) of C2C12 cells.
(A) Representative whole-cell sodium current traces. The peak current density of the I_{Na} in miR-142a-3p overexpression and NC groups were similar, while the peak current density of the I_{Na} in the miR-142a-3p knockdown group was lower than that in the NC group. (B) Relationship of peak current densities and voltage. (C) The voltage clamp protocol. Data are expressed as mean ± SEM (NC: Negative control group, n = 8; miR-142a-3p mimics: miR-142a-3p overexpression group, n = 9; miR-142a-3p inhibitor: miR-142a-3p knockdown group, n = 8). *P <0.05, **P <0.01, *vs.* NC (two-tailed Student's t-test).

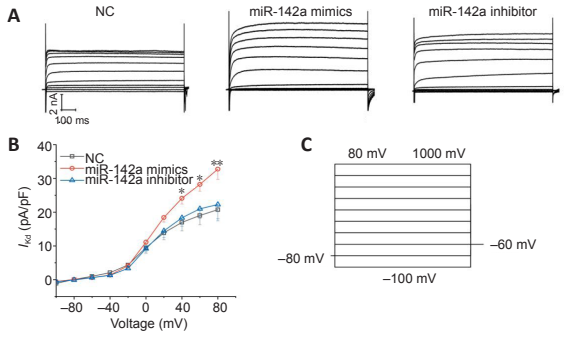

Figure 4 | Overexpression of miR-142a-3p decreases the potassium ion channel currents (I_{Kd}) of C2C12 cells.
(A) Representative whole-cell potassium current traces. The peak currents density of the I_{Kd} in miR-142a-3p overexpression group was higher than that in NC group, whereas in the miR-142a-3p knockdown group, the currents densities of the I_{Kd} in miR-142a-3p knockdown and NC groups were similar. (B) Relationship of peak current densities and voltage. (C) The voltage clamp protocol. Data are expressed as mean ± SEM (NC: Negative control group, n = 8; miR-142a-3p mimics: miR-142a-3p overexpression group, n = 7; miR-142a-3p inhibitor: miR-142a-3p knockdown group, n = 7). *P <0.05, **P <0.01, *vs.* NC group (two-tailed Student's t-test).

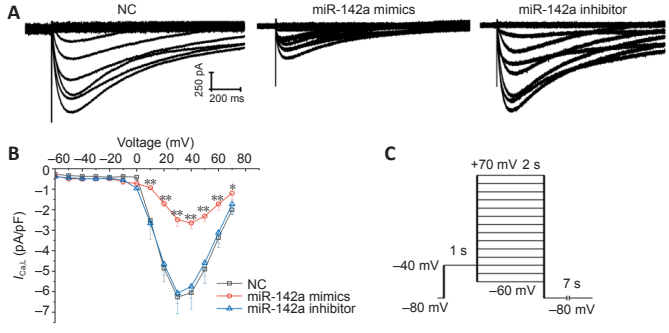

Figure 5 | Knockdown of miR-142a-3p decreases the L-type calcium channel ($I_{Ca,L}$) current density of C2C12 cells.
(A) Representative $I_{Ca,L}$ current traces. In the miR-142a-3p overexpression group, the peak current density of $I_{Ca,L}$ was lower than that in NC, while the peak current densities of $I_{Ca,L}$ in miR-142a-3p knockdown and NC groups were similar. (B) Relationship of peak current densities and voltage. (C) The voltage clamp protocol. Data are expressed as mean ± SEM (NC: negative control group, n = 8; miR-142a-3p mimics: miR-142a-3p overexpression group, n = 7; miR-142a-3p inhibitor: miR-142a-3p knockdown group, n = 8). *P <0.05, **P < 0.01, *vs.* NC (two-tailed Student's t-test).

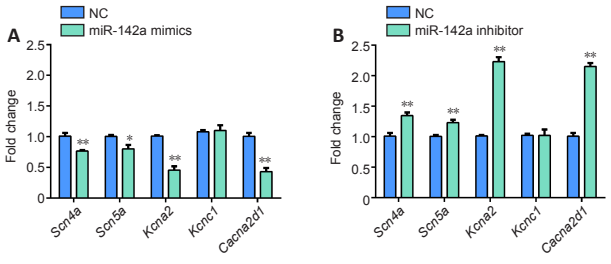

Figure 6 | MiR-142a-3p affects the expression of ion channel-related genes in C2C12 cells.
(A, B) Quantitative real-time reverse transcription-polymerase chain reaction was implemented to detect the expression of ion channel-related genes in miR-142a mimics (A) and miR-142a inhibitor group (B). Relative gene expression was normalized by fold change. Data are expressed as mean ± SEM (n = 3/group). *P <0.05, **P <0.01, *vs.* NC (two-tailed Student's t-test). miR-142a inhibitor: miR-142a-3p knockdown group; miR-142a mimics: miR-142a-3p overexpression group; NC: negative control group.

Discussion

Ion channels are critical to the function of excitable cells and they have been found to be regulated by miRNAs in many organs, including skeletal muscles. miR-142a-3p and many ion channel coding genes have been found to be highly differently expressed in skeletal muscle after denervation (**Additional Table 1**) (Weng et al., 2018). The predicted target genes of miR-142a-3p showed a high degree of participation in the binding of metals, cations and ions (**Additional Figure 1**). Thus, we propose that miR-142a-3p may regulate skeletal muscle electrophysiology.

In this study, whole-cell currents were recorded after 7-day differentiation. Our results showed that in the miR-142a-3p overexpression group cells had smaller membrane capacitance, higher potassium current density and lower L-calcium current density; in contrast, the miR-142a-3p knockdown group exhibited greater membrane capacitance and lower sodium ion channel current density.

Our experiments showed that miR-142a affected cell fusion, and the miR-142a overexpression group had more mature, differentiated cells. The differing development level of myotubes between the different groups could be associated with differences in the expression of ion channels (Moody and Bosma, 2005). In order to analyze the possible mechanism of miR-142a-3p in regulating ion channel current, we predicted the target genes of miR-142a-3p. We showed that miR-142a-3p may target *Scn4a*, *Scn5a*, *Kcnc1*, *Kcna2*, and *Cacna2d1*. Scn5a was one of the few ion channel coding genes with increased expression. There was also evidence that expression of the voltage-gated sodium channel, Nav1.5, appeared together with the fibrillation potentials in the early stage of denervation atrophy, and that inhibition of Nav1.5 could weaken fibrillation potentials (Sekiguchi et al., 2012). There is no direct evidence that miR-142a targets Scn5a, but some studies have found that ectopic expression of miR-142-3p inhibited the expression of Tbx5, and Tbx5 drives Scn5a expression to influence the functioning of the cardiac conduction system (Arnolds et al., 2012; Chen et al., 2017). We also searched the gene expression files of nine human muscle diseases. Compared with normal human skeletal muscle, *Scn4a*, *Kcna1*, *Cacna1a* and *Cacna1b* are generally up-regulated, and *Kcna2*, *Kcna3* and *Cacna1c* are down-regulated in a variety of diseases (National Institutes of Health, 2005) (**Additional Table 2**). miR-142a-3p targets ion channel genes and inhibits their expression, which may be of significance in the development of skeletal muscle diseases.

We found that knocking down miR-142a-3p can reduce sodium currents density. The action potentials of muscles, as in nerves, are initiated with the opening of sodium channels. Sodium currents cause rapid depolarization of the membrane and the propagation of potential and electrical input from negative to slightly positive passes along the fiber (Hodgkin and Huxley, 1952; Adrian et al., 1970; Hudson et al., 1995). Jurkat-Rott et al. (2000) studied periodic paralysis and found that decreased inward sodium currents in skeletal muscle can lead to low excitability of the fibrous membrane and cause muscle weakness. Therefore, knocking down miR-142a-3p can reduce sodium current density, which may further affect cell excitability. In addition, changes in ion channel expression may have important effects on the electrophysiological properties of a cell. The mouse model showed that decreased expression of Scn5a in the heart would slow down ventricular conduction (van Veen et al., 2005), whereas overexpression of Scn5a would enhance AV conduction, which mimics the human syndrome of enhanced atrioventricular nodal conduction (Liu et al., 2015). The possible regulatory effects of miR-142a-3p on *Scn4a* and *Scn5a* may also affect cell excitability and electrical conduction.

Up-regulation of miR-142a-3p increased the current density of I_{Kd}, suggesting that the cells are more easily repolarized, resulting in a shorter time course of their action potentials. Since I_{Kd} are responsible for the repolarization phase of the action potential, the increase in delayed outward current helps to establish the excitement cycle and shorten the action potential (Moody and Bosma, 2005). Therefore, the elevated potassium current in C2C12 may hasten their return to a resting state, maintain the stability of the cell state and resist external stimuli.

Calcium current density was reduced by overexpression of miR-142a-3p, which may be related to the excitation-contraction coupling. Two types of voltage-gated calcium channel (VDCC) are found in skeletal muscle: 1) L-type VDCC generated by the CaV1.1/α1s subunit, which plays a key role in excitatory contraction (Tanabe et al., 1993) and 2) t-type VDCC, generated by the CaV3.2/α1H subunit, which is important in muscle development (Cognard et al., 1986). This experiment recorded L-type VDCC currents, and the L-type Ca^{2+} channel, 4-1-dihydropyridine receptor complex was used as an excitation-contraction coupling voltage sensor (Tanabe et al., 1988). During membrane depolarization, the conformational change of dihydropyridine receptor is coupled with ryanodine receptor 1, allowing the calcium ions to enter the sarcoplasm via ryanodine receptor 1 to initiate contraction (Endo, 1977; Lee et al., 2006). Therefore, $I_{Ca,L}$ currents are very important for skeletal muscle excitation-contraction coupling, and reduced $I_{Ca,L}$ currents in C2C12 may have similar effects to skeletal muscle. Cacna2d1 encodes the α2 and δ1 subunits of the $I_{Ca,L}$ (Arikkath and Campbell, 2003) and Schug et al. (2013) found that miR-142a-3p targets Cacna2d1 in mice liver cells by high-throughput sequencing with crosslinking-immunoprecipitation. However, it is not clear that miR-142a-3p regulates $I_{Ca,L}$ by targeting *Cacna2d* in muscle cells. These miRNA/ion channel mechanisms are also valuable for explaining the adaptive changes of muscle cell excitation-contraction coupling after denervation.

Comparing our previous work on miR-34c-5p with this study (Jin et al., 2020), we found that both miR-34c-5p and miR-142a-3p are significantly up-regulated in denervated skeletal muscle, whereas their effects on specific currents are totally different. It is interesting that one side-regulation on ion channels was observed with each miRNA but to different effects. For sodium channels, there is no significant change in I_{Na} when miR-34c-5p is overexpressed or knocked down, whereas knockdown of miR-142a-3p can reduce I_{Na}. For the delayed rectified potassium current, knockdown of miR-34c-5p and overexpression of miR-142a-3p can increase I_{Kd}. For the L-type calcium current, overexpression of miR-34c-5p can increase $I_{Ca,L}$ current, while overexpression of miR-142a-3p can reduce the $I_{Ca,L}$ current. Similar phenomena also appear in other tissues. For example, overexpression of miR-370-3p reduces the hyperpolarization-activated channel current, but the knockdown group was not different from the control group (Yanni et al., 2020). The possible reason for this phenomenon is that different miRNAs have different regulatory targets and thus perform different functions.

In summary, we have studied the regulatory effect of miR-142a-3p on C2C12 ion channels. We used the C2C12 cell line, whose physiological characteristics may be slightly different from true skeletal muscle cells, but the results still suggest that miRNAs function as regulators of ion channels. The specific channel subtypes and regulatory mechanisms of miR-142a-3p in regulating whole-cell sodium, potassium and calcium channels need further investigation and this is the direction of our follow-up experiments.

Author contributions: *Study conceptualization, methodology, and data analysis: XFY; data curation, andoriginal draft preparation: XYG; visualization, and investigation: BJ; supervision: ZDQ. All authors*

approved the final version of the manuscript.

Conflicts of interest: *The authors declare that there is no conflict of interests.*

Financial support: *This study was supported by the National Natural Science Foundation of China, Nos. 82072162, 81971177; and Beijing Municipal Natural Science Foundation of China, No. 7192215 (all to XFY). The funding sources had no role in study conception and design, data analysis or interpretation, paper writing or deciding to submit this paper for publication.*

Institutional review board statement: *The study was approved by the Animal Ethics Committee of Peking University in July 2020 (approval No. LA2017128).*

Data sharing statement: *Datasets analyzed during the current study are available from the corresponding author on reasonable request.*

Plagiarism check: *Checked twice by iThenticate.*

Peer review: *Externally peer reviewed.*

Open peer reviewer: *Yao Tong, The Scripps Research Institute, USA.*

Additional files:

Additional Table 1: *Differentially expressed ion channel coding genes in skeletal muscle after denervation.*

Additional Table 2: *Differential expression of ion channel genes in multiple human muscle diseases.*

Additional Figure 1: *Gene Ontology (GO) analysis of miR-142a-3p predictive target mRNAs at each time point.*

Additional file 1: *Open peer review report 1.*

References

Adrian RH, Chandler WK, Hodgkin AL (1970) Voltage clamp experiments in striated muscle fibres. J Physiol 208:607-644.

Arikkath J, Campbell KP (2003) Auxiliary subunits: essential components of the voltage-gated calcium channel complex. Curr Opin Neurobiol 13:298-307.

Arnolds DE, Liu F, Fahrenbach JP, Kim GH, Schillinger KJ, Smemo S, McNally EM, Nobrega MA, Patel VV, Moskowitz IP (2012) TBX5 drives Scn5a expression to regulate cardiac conduction system function. J Clin Invest 122:2509-2518.

Baroukh N, Ravier MA, Loder MK, Hill EV, Bounacer A, Scharfmann R, Rutter GA, Van Obberghen E (2007) MicroRNA-124a regulates Foxa2 expression and intracellular signaling in pancreatic beta-cell lines. J Biol Chem 282:19575-19588.

Beam KG, Knudson CM, Powell JA (1986) A lethal mutation in mice eliminates the slow calcium current in skeletal muscle cells. Nature 320:168-170.

Chemello F, Grespi F, Zulian A, Cancellara P, Hebert-Chatelain E, Martini P, Bean C, Alessio E, Buson L, Bazzega M, Armani A, Sandri M, Ferrazza R, Laveder P, Guella G, Reggiani C, Romualdi C, Bernardi P, Scorrano L, Cagnin S, et al. (2019) Transcriptomic analysis of single isolated myofibers identifies miR-27a-3p and miR-142-3p as regulators of metabolism in skeletal muscle. Cell Rep 26:3784-3797.e3788.

Chen ZY, Chen F, Cao N, Zhou ZW, Yang HT (2017) miR-142-3p contributes to early cardiac fate decision of embryonic stem cells. Stem Cells Int 2017:1769298.

Cognard C, Lazdunski M, Romey G (1986) Different types of Ca^{2+} channels in mammalian skeletal muscle cells in culture. Proc Natl Acad Sci U S A 83:517-521.

Endo M (1977) Calcium release from the sarcoplasmic reticulum. Physiol Rev 57:71-108.

Hodgkin AL, Huxley AF (1952) The components of membrane conductance in the giant axon of Loligo. J Physiol 116:473-496.

Hudson AJ, Ebers GC, Bulman DE (1995) The skeletal muscle sodium and chloride channel diseases. Brain 118 (Pt 2):547-563.

Jin B, Gu X, Li D, Qi Z, Jiang B, Yin X (2020) Effects of miR-34c-5p on sodium, potassium, and calcium channel currents in C2C12 myotubes. Cell Mol Neurobiol 40:1223-1230.

Jurkat-Rott K, Mitrovic N, Hang C, Kouzmekine A, Iaizzo P, Herzog J, Lerche H, Nicole S, Vale-Santos J, Chauveau D, Fontaine B, Lehmann-Horn F (2000) Voltage-sensor sodium channel mutations cause hypokalemic periodic paralysis type 2 by enhanced inactivation and reduced current. Proc Natl Acad Sci U S A 97:9549-9554.

Kaduthanam S, Gade S, Meister M, Brase JC, Johannes M, Dienemann H, Warth A, Schnabel PA, Herth FJ, Sültmann H, Muley T, Kuner R (2013) Serum miR-142-3p is associated with early relapse in operable lung adenocarcinoma patients. Lung Cancer 80:223-227.

Kramer NJ, Wang WL, Reyes EY, Kumar B, Chen CC, Ramakrishna C, Cantin EM, Vonderfecht SL, Taganov KD, Chau N, Boldin MP (2015) Altered lymphopoiesis and immunodeficiency in miR-142 null mice. Blood 125:3720-3730.

Kubo Y (1991) Comparison of initial stages of muscle differentiation in rat and mouse myoblastic and mouse mesodermal stem cell lines. J Physiol 442:743-759.

Lee EH, Kim DH, Allen PD (2006) Interplay between intra- and extracellular calcium ions. Mol Cells 21:315-329.

Liu GX, Remme CA, Boukens BJ, Belardinelli L, Rajamani S (2015) Overexpression of SCN5A in mouse heart mimics human syndrome of enhanced atrioventricular nodal conduction. Heart Rhythm 12:1036-1045.

Mandolesi G, De Vito F, Musella A, Gentile A, Bullitta S, Fresegna D, Sepman H, Di Sanza C, Haji N, Mori F, Buttari F, Perlas E, Ciotti MT, Hornstein E, Bozzoni I, Presutti C, Centonze D (2017) miR-142-3p is a key regulator of IL-1β-dependent synaptopathy in neuroinflammation. J Neurosci 37:546-561.

Manna I, De Benedittis S, Iaccino E, Quattrone A, Quattrone A (2021) Diagnostic and therapeutic potential of exosomal miRNAs in Alzheimer's disease. Neural Regen Res 16:2217-2218.

Moody WJ, Bosma MM (2005) Ion channel development, spontaneous activity, and activity-dependent development in nerve and muscle cells. Physiol Rev 85:883-941.

Nakada T, Kashihara T, Komatsu M, Kojima K, Takeshita T, Yamada M (2018) Physical interaction of junctophilin and the Ca(V)1.1 C terminus is crucial for skeletal muscle contraction. Proc Natl Acad Sci U S A 115:4507-4512.

National Institutes of Health (2005) GSE3307. https://www.ncbi.nlm.nih.gov/geo/query/acc.cgi?acc=GSE3307. Accessed May 20, 2021.

Nimmo R, Ciau-Uitz A, Ruiz-Herguido C, Soneji S, Bigas A, Patient R, Enver T (2013) MiR-142-3p controls the specification of definitive hemangioblasts during ontogeny. Dev Cell 26:237-249.

Pardo LA, Stühmer W (2008) Eag1: an emerging oncological target. Cancer Res 68:1611-1613.

Pietrzykowski AZ, Friesen RM, Martin GE, Puig SI, Nowak CL, Wynne PM, Siegelmann HT, Treistman SN (2008) Posttranscriptional regulation of BK channel splice variant stability by miR-9 underlies neuroadaptation to alcohol. Neuron 59:274-287.

Saugstad JA (2010) MicroRNAs as effectors of brain function with roles in ischemia and injury, neuroprotection, and neurodegeneration. J Cereb Blood Flow Metab 30:1564-1576.

Sekiguchi K, Kanda F, Mitsui S, Kohara N, Chihara K (2012) Fibrillation potentials of denervated rat skeletal muscle are associated with expression of cardiac-type voltage-gated sodium channel isoform Nav1.5. Clin Neurophysiol 123:1650-1655.

Shi L, Ko ML, Ko GY (2009) Rhythmic expression of microRNA-26a regulates the L-type voltage-gated calcium channel alpha1C subunit in chicken cone photoreceptors. J Biol Chem 284:25791-25803.

Shrestha A, Carraro G, El Agha E, Mukhametshina R, Chao CM, Rizvanov A, Barreto G, Bellusci S (2015) Generation and validation of miR-142 knock out mice. PLoS One 10:e0136913.

Tanabe T, Beam KG, Powell JA, Numa S (1988) Restoration of excitation-contraction coupling and slow calcium current in dysgenic muscle by dihydropyridine receptor complementary DNA. Nature 336:134-139.

Tanabe T, Mikami A, Niidome T, Numa S, Adams BA, Beam KG (1993) Structure and function of voltage-dependent calcium channels from muscle. Ann N Y Acad Sci 707:81-86.

van Veen TA, Stein M, Royer A, Le Quang K, Charpentier F, Colledge WH, Huang CL, Wilders R, Grace AA, Escande D, de Bakker JM, van Rijen HV (2005) Impaired impulse propagation in Scn5a-knockout mice: combined contribution of excitability, connexin expression, and tissue architecture in relation to aging. Circulation 112:1927-1935.

Weng J, Zhang P, Yin X, Jiang B (2018) The whole transcriptome involved in denervated muscle atrophy following peripheral nerve injury. Front Mol Neurosci 11:69.

Yang B, Lin H, Xiao J, Lu Y, Luo X, Li B, Zhang Y, Xu C, Bai Y, Wang H, Chen G, Wang Z (2007) The muscle-specific microRNA miR-1 regulates cardiac arrhythmogenic potential by targeting GJA1 and KCNJ2. Nat Med 13:486-491.

Yanni J, D'Souza A, Wang Y, Li N, Hansen BJ, Zakharkin SO, Smith M, Hayward C, Whitson BA, Mohler PJ, Janssen PML, Zeef L, Choudhury M, Zi M, Cai X, Logantha S, Nakao S, Atkinson A, Petkova M, Doris U, et al. (2020) Silencing miR-370-3p rescues funny current and sinus node function in heart failure. Sci Rep 10:11279.

Zeng L, Jiang HL, Ashraf GM, Li ZR, Liu R (2021) MicroRNA and mRNA profiling of cerebral cortex in a transgenic mouse model of Alzheimer's disease by RNA sequencing. Neural Regen Res 16:2099-2108.

P-Reviewer: Tong Y; C-Editor: Zhao M; S-Editors: Yu J, Li CH;
L-Editors: Yu J, Song LP; T-Editor: Jia Y

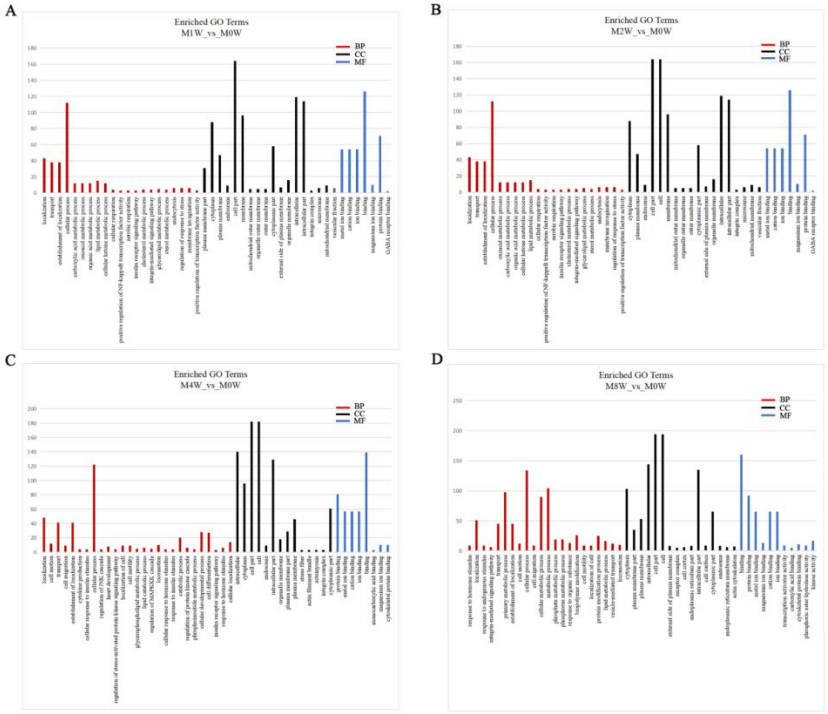

Additional Figure 1 Gene Ontology (GO) analysis of miR-142a-3p predictive target mRNAs at each time point.

Directed acyclic graph showed the significant BP, CC, and MF. *y*-axis indicate the numbers of genes for each GO term. (A) 1 week *vs*. 0 week. (B) 2 weeks *vs*. 0 week. (C) 4 weeks *vs*. 0 week. (D) 8 weeks *vs*. 0 week. BP: Biological process; CC: cellular component; MF: molecular function.

Additional Table 1 Differentially expressed ion channel coding genes in skeletal muscle after denervation

Gene ID	Gene name	INJ FPKM	CON FPKM	Log2 fold change	*P*-value	Channel type
1 wk *vs.* 0 wk						
ENSMUSG00000034810	*Scn7a*	10.2123	4.54198	1.16892	5.00E-05	Sodium channel
ENSMUSG00000019194	*Scn1b*	185.984	400.765	-1.10758	5.00E-05	Sodium channel
ENSMUSG00000001027	*Scn4a*	57.7301	139.201	-1.26978	5.00E-05	Sodium channel
ENSMUSG00000049281	*Scn3b*	1.26093	0.335519	1.91002	5.00E-05	Sodium channel
ENSMUSG00000032511	*Scn5a*	6.63433	0.121698	5.76858	5.00E-05	Sodium channel
ENSMUSG00000046480	*Scn4b*	10.8807	142.79	-3.71406	5.00E-05	Sodium channel
ENSMUSG00000070304	*Scn2b*	0.347979	1.11337	-1.67786	0.00055	Sodium channel
ENSMUSG00000040724	*Kcna2*	0.462553	0.93962	-1.02246	5.00E-05	Potassium channel
ENSMUSG00000023243	*Kcnk5*	17.4945	1.30671	3.74289	5.00E-05	Potassium channel
ENSMUSG00000090122	*Kcne1l*	2.44987	0.507395	2.27152	5.00E-05	Potassium channel
ENSMUSG00000028033	*Kcnq5*	5.93443	2.40914	1.30059	5.00E-05	Potassium channel
ENSMUSG00000045246	*Kcng4*	0.181382	5.83865	-5.00853	5.00E-05	Potassium channel
ENSMUSG00000027827	*Kcnab1*	0.731955	1.61284	-1.13978	0.00065	Potassium channel
ENSMUSG00000002908	*Kcnn1*	2.65705	6.47878	-1.2859	5.00E-05	Potassium channel
ENSMUSG00000042529	*Kcnj12*	4.50593	31.1286	-2.78835	5.00E-05	Potassium channel
ENSMUSG00000045534	*Kcna5*	3.66456	11.2919	-1.62358	5.00E-05	Potassium channel
ENSMUSG00000062785	*Kcnc3*	0.524387	2.79554	-2.41442	5.00E-05	Potassium channel
ENSMUSG00000030247	*Kcnj8*	3.98421	9.88858	-1.31147	0.0001	Potassium channel
ENSMUSG00000038201	*Kcna7*	4.11071	58.5853	-3.83308	5.00E-05	Potassium channel
ENSMUSG00000000794	*Kcnn3*	18.8122	0.853325	4.46243	5.00E-05	Potassium channel
ENSMUSG00000028033	*Kcnq5*	6.29738	1.91864	1.71466	5.00E-05	Potassium channel
ENSMUSG00000058975	*Kcnc1*	1.10461	20.3304	-4.20203	5.00E-05	Potassium channel
ENSMUSG00000027895	*Kcnc4*	18.9838	28.7616	-0.599376	0.00275	Potassium channel
ENSMUSG00000096146	*Kcnj11*	28.7368	61.0577	-1.08727	5.00E-05	Potassium channel
ENSMUSG00000033998	*Kcnk1*	0.136612	0.612726	-2.16516	0.0003	Potassium channel
ENSMUSG00000054477	*Kcnn2*	0.212113	0.985792	-2.21645	5.00E-05	Potassium channel
ENSMUSG00000041695	*Kcnj2*	9.70121	23.7332	-1.29067	5.00E-05	Potassium channel
ENSMUSG00000038319	*Kcnh2*	0.286328	0.813449	-1.50638	0.00045	Potassium channel
ENSMUSG00000078815	*Cacng6*	30.5703	74.4878	-1.28487	5.00E-05	Calcium channel
ENSMUSG00000069806	*Cacng7*	3.23436	7.52438	-1.21809	5.00E-05	Calcium channel
ENSMUSG00000020882	*Cacnb1*	16.3872	105.691	-2.68921	5.00E-05	Calcium channel
ENSMUSG00000020722	*Cacng1*	851.169	224.509	1.92267	5.00E-05	Calcium channel
2 wk *vs.* 0 wk						
ENSMUSG00000019194	*Scn1b*	236.916	400.765	-0.758384	0.0004	Sodium channel
ENSMUSG00000057182	*Scn3a*	1.20077	0.152791	2.97434	0.00095	Sodium channel
ENSMUSG00000001027	*Scn4a*	63.965	139.201	-1.12182	5.00E-05	Sodium channel
ENSMUSG00000049281	*Scn3b*	1.06145	0.335519	1.66157	0.00015	Sodium channel
ENSMUSG00000032511	*Scn5a*	8.63138	0.121698	6.14822	5.00E-05	Sodium channel
ENSMUSG00000046480	*Scn4b*	11.4717	142.79	-3.63775	5.00E-05	Sodium channel
ENSMUSG00000070304	*Scn2b*	0.381914	1.11337	-1.54361	0.00075	Sodium channel
ENSMUSG00000040724	*Kcna2*	0.277742	0.93962	-1.75833	5.00E-05	Potassium channel
ENSMUSG00000047976	*Kcna1*	0.969303	2.1224	-1.13068	0.00035	Potassium channel
ENSMUSG00000023243	*Kcnk5*	19.257	1.30671	3.88137	5.00E-05	Potassium channel
ENSMUSG00000090122	*Kcne1l*	4.65046	0.507395	3.19619	5.00E-05	Potassium channel
ENSMUSG00000028033	*Kcnq5*	5.87395	2.40914	1.28582	0.00025	Potassium channel
ENSMUSG00000045246	*Kcng4*	0.242834	5.83865	-4.58759	5.00E-05	Potassium channel

ENSMUSG00000027827	*Kcnab1*	0.696459	1.61284	-1.21149	0.0004	Potassium channel
ENSMUSG00000002908	*Kcnn1*	2.72504	6.47878	-1.24945	5.00E-05	Potassium channel
ENSMUSG00000042529	*Kcnj12*	5.88353	31.1286	-2.40349	5.00E-05	Potassium channel
ENSMUSG00000045534	*Kcna5*	4.52864	11.2919	-1.31814	5.00E-05	Potassium channel
ENSMUSG00000062785	*Kcnc3*	1.2178	2.79554	-1.19885	0.0001	Potassium channel
ENSMUSG00000030247	*Kcnj8*	5.08842	9.88858	-0.958546	0.0003	Potassium channel
ENSMUSG00000038201	*Kcna7*	6.22924	58.5853	-3.23341	5.00E-05	Potassium channel
ENSMUSG00000000794	*Kcnn3*	29.7446	0.853325	5.12339	5.00E-05	Potassium channel
ENSMUSG00000028033	*Kcnq5*	7.60192	1.91864	1.98628	5.00E-05	Potassium channel
ENSMUSG00000058975	*Kcnc1*	2.07504	20.3304	-3.29243	5.00E-05	Potassium channel
ENSMUSG00000027895	*Kcnc4*	14.1031	28.7616	-1.02813	5.00E-05	Potassium channel
ENSMUSG00000096146	*Kcnj11*	18.984	61.0577	-1.68539	5.00E-05	Potassium channel
ENSMUSG00000033998	*Kcnk1*	0.0883864	0.612726	-2.79335	0.00025	Potassium channel
ENSMUSG00000054477	*Kcnn2*	0.221758	0.985792	-2.15229	5.00E-05	Potassium channel
ENSMUSG00000041695	*Kcnj2*	10.3367	23.7332	-1.19913	5.00E-05	Potassium channel
ENSMUSG00000038319	*Kcnh2*	0.180432	0.813449	-2.17259	0.00015	Potassium channel
ENSMUSG00000063142	*Kcnma1*	4.32059	10.2465	-1.24583	0.001	Potassium channel
ENSMUSG00000078815	*Cacng6*	30.149	74.4878	-1.30489	5.00E-05	Calcium channel
ENSMUSG00000069806	*Cacng7*	2.99559	7.52438	-1.32873	5.00E-05	Calcium channel
ENSMUSG00000020882	*Cacnb1*	21.8478	105.691	-2.27429	5.00E-05	Calcium channel
ENSMUSG00000020722	*Cacng1*	481.484	224.509	1.10071	5.00E-05	Calcium channel
4 wk *vs*. 0 wk						
ENSMUSG00000034810	*Scn7a*	8.48514	4.54198	0.901618	0.0001	Sodium channel
ENSMUSG00000019194	*Scn1b*	189.765	400.765	-1.07854	5.00E-05	Sodium channel
ENSMUSG00000057182	*Scn3a*	1.50615	0.152791	3.30124	0.00045	Sodium channel
ENSMUSG00000001027	*Scn4a*	37.6173	139.201	-1.88771	5.00E-05	Sodium channel
ENSMUSG00000032511	*Scn5a*	7.79094	0.121698	6.00042	5.00E-05	Sodium channel
ENSMUSG00000046480	*Scn4b*	7.71076	142.79	-4.21088	5.00E-05	Sodium channel
ENSMUSG00000070304	*Scn2b*	0.258586	1.11337	-2.10622	5.00E-05	Sodium channel
ENSMUSG00000040724	*Kcna2*	0.428762	0.93962	-1.1319	0.0001	Potassium channel
ENSMUSG00000023243	*Kcnk5*	10.9096	1.30671	3.06158	5.00E-05	Potassium channel
ENSMUSG00000090122	*Kcne1l*	2.23034	0.507395	2.13609	5.00E-05	Potassium channel
ENSMUSG00000045246	*Kcng4*	0.3204	5.83865	-4.18769	5.00E-05	Potassium channel
ENSMUSG00000002908	*Kcnn1*	2.19654	6.47878	-1.56049	5.00E-05	Potassium channel
ENSMUSG00000042529	*Kcnj12*	4.04445	31.1286	-2.94423	5.00E-05	Potassium channel
ENSMUSG00000045534	*Kcna5*	2.04818	11.2919	-2.46287	5.00E-05	Potassium channel
ENSMUSG00000062785	*Kcnc3*	1.09363	2.79554	-1.354	0.00195	Potassium channel
ENSMUSG00000030247	*Kcnj8*	4.94743	9.88858	-0.999086	0.00045	Potassium channel
ENSMUSG00000038201	*Kcna7*	5.81574	58.5853	-3.3325	5.00E-05	Potassium channel
ENSMUSG00000000794	*Kcnn3*	30.0514	0.853325	5.13819	5.00E-05	Potassium channel
ENSMUSG00000028033	*Kcnq5*	5.60965	1.91864	1.54782	5.00E-05	Potassium channel
ENSMUSG00000058975	*Kcnc1*	2.36221	20.3304	-3.10543	5.00E-05	Potassium channel
ENSMUSG00000027895	*Kcnc4*	9.77607	28.7616	-1.55682	5.00E-05	Potassium channel
ENSMUSG00000096146	*Kcnj11*	14.4349	61.0577	-2.08061	5.00E-05	Potassium channel
ENSMUSG00000033998	*Kcnk1*	0.105185	0.612726	-2.54231	0.0004	Potassium channel
ENSMUSG00000054477	*Kcnn2*	0.27786	0.985792	-1.82693	5.00E-05	Potassium channel
ENSMUSG00000041695	*Kcnj2*	11.5332	23.7332	-1.04112	5.00E-05	Potassium channel
ENSMUSG00000047959	*Kcna3*	0.5274	0.164098	1.68434	0.00255	Potassium channel
ENSMUSG00000078815	*Cacng6*	21.6355	74.4878	-1.7836	5.00E-05	Calcium channel
ENSMUSG00000069806	*Cacng7*	3.43521	7.52438	-1.13117	5.00E-05	Calcium channel

ENSMUSG00000024112	*Cacna1h*	0.475177	0.979642	-1.04379	0.0003	Calcium channel
ENSMUSG00000020882	*Cacnb1*	16.953	105.691	-2.64024	5.00E-05	Calcium channel
8 wk *vs*. 0 wk						
ENSMUSG00000019194	*Scn1b*	162.512	400.765	-1.30221	5.00E-05	Sodium channel
ENSMUSG00000057182	*Scn3a*	2.74497	0.152791	4.16716	5.00E-05	Sodium channel
ENSMUSG00000075318	*Scn2a1*	0.950277	0.200929	2.24166	0.0017	Sodium channel
ENSMUSG00000001027	*Scn4a*	39.0421	139.201	-1.83407	5.00E-05	Sodium channel
ENSMUSG00000032511	*Scn5a*	7.13261	0.121698	5.87306	5.00E-05	Sodium channel
ENSMUSG00000046480	*Scn4b*	8.21354	142.79	-4.11975	5.00E-05	Sodium channel
ENSMUSG00000070304	*Scn2b*	0.36137	1.11337	-1.62338	0.003	Sodium channel
ENSMUSG00000040724	*Kcna2*	0.26861	0.93962	-1.80656	5.00E-05	Potassium channel
ENSMUSG00000047976	*Kcna1*	1.0037	2.1224	-1.08037	0.0004	Potassium channel
ENSMUSG00000023243	*Kcnk5*	5.96463	1.30671	2.19049	5.00E-05	Potassium channel
ENSMUSG00000090122	*Kcne1l*	1.71599	0.507395	1.75786	5.00E-05	Potassium channel
ENSMUSG00000045246	*Kcng4*	0.332686	5.83865	-4.1334	5.00E-05	Potassium channel
ENSMUSG00000063142	*Kcnma1*	2.45397	6.17737	-1.33187	0.00155	Potassium channel
ENSMUSG00000002908	*Kcnn1*	1.68307	6.47878	-1.94462	5.00E-05	Potassium channel
ENSMUSG00000042529	*Kcnj12*	4.24837	31.1286	-2.87326	5.00E-05	Potassium channel
ENSMUSG00000045534	*Kcna5*	2.66115	11.2919	-2.08517	5.00E-05	Potassium channel
ENSMUSG00000062785	*Kcnc3*	1.43477	2.79554	-0.96231	0.00185	Potassium channel
ENSMUSG00000030247	*Kcnj8*	4.409	9.88858	-1.16531	5.00E-05	Potassium channel
ENSMUSG00000038201	*Kcna7*	6.9193	58.5853	-3.08184	5.00E-05	Potassium channel
ENSMUSG00000000794	*Kcnn3*	27.9025	0.853325	5.03116	5.00E-05	Potassium channel
ENSMUSG00000028033	*Kcnq5*	7.32761	1.91864	1.93326	5.00E-05	Potassium channel
ENSMUSG00000058975	*Kcnc1*	2.76581	20.3304	-2.87787	5.00E-05	Potassium channel
ENSMUSG00000027895	*Kcnc4*	16.1055	28.7616	-0.836586	5.00E-05	Potassium channel
ENSMUSG00000096146	*Kcnj11*	18.7055	61.0577	-1.70671	5.00E-05	Potassium channel
ENSMUSG00000028631	*Kcnq4*	9.96216	5.5618	0.840907	5.00E-05	Potassium channel
ENSMUSG00000033998	*Kcnk1*	0.0923963	0.612726	-2.72934	0.0001	Potassium channel
ENSMUSG00000054477	*Kcnn2*	0.323318	0.985792	-1.60833	5.00E-05	Potassium channel
ENSMUSG00000041695	*Kcnj2*	9.10985	23.7332	-1.3814	5.00E-05	Potassium channel
ENSMUSG00000038319	*Kcnh2*	0.301894	0.813449	-1.43001	0.00155	Potassium channel
ENSMUSG00000050556	*Kcnb1*	4.52293	9.49624	-1.0701	5.00E-05	Potassium channel
ENSMUSG00000078815	*Cacng6*	19.2107	74.4878	-1.9551	5.00E-05	Calcium channel
ENSMUSG00000069806	*Cacng7*	3.65829	7.52438	-1.0404	5.00E-05	Calcium channel
ENSMUSG00000020882	*Cacnb1*	15.273	105.691	-2.79079	5.00E-05	Calcium channel

The data of CON group was from Weng et al. (2018). CON: Control; INJ: injured; FPKM: fragments per kilobase of exon model per million mapped fragments. Cacna2d1: Calcium voltage-gated channel auxiliary subunit alpha2delta 1; GAPDH: glyceraldehyde-3-phosphate dehydrogenase; Kcna2: potassium voltage-gated channel subfamily A member 2; Kcnc1: potassium voltage-gated channel subfamily C member 1; Scn4a: sodium voltage-gated channel alpha subunit 4.

Additional Table 2 Differential expression of ion channel genes in multiple human muscle diseases

	Becker muscular dystrophy	Duchenne muscular dystrophy	Emery Dreifuss muscular dystrophy	Juvenile dermatomyositis	Dysferlinopathy	Amyotophic lateral sclerosis	Calpainopathy	Fukutin-related protein mutation	Acute quadriplegic myopathy
SCN4A	↑	↑	↑	↑	↑	↑	↑	↑	↑
KCNA1	↑	↑	↑	↑	↑	↑	↑	↑	↑
KCNA2	↑	↓	↑	↓	↑	↑	↑	↓	↑
KCNA3	↓	↑	↓	↑	↑	↑	↑	↑	↑
CACNA1A	↑	↑	↑	↑	↑	↑	↑	↑	↑
CACNA1B	↑	↑	↑	↑	↑	↑	↑	↑	↑
CACNA1C	↓	↓	↑	↑	↑	↑	↑	↑	↑

↑: Upregulation; ↓: downregulation. CACNA: Calcium voltage-gated channel auxiliary; KCNA: potassium voltage-gated channel subfamily A member; SCN4A: sodium voltage-gated channel alpha subunit 4.